Human Cytomegalovirus Protease Complexes Its Substrate Recognition Sequences in an Extended Peptide Conformation[†,‡]

Steven R. LaPlante,* Norman Aubry, Pierre R. Bonneau, Dale R. Cameron, Lisette Lagacé, Marie-Josée Massariol, Hélène Montpetit, Céline Plouffe, and Stephen H. Kawai

Departments of Chemistry and Biological Sciences, Bio-Méga Research Division, Boehringer Ingelheim (Canada) Ltd., Laval, Québec H7S 2G5, Canada

Bruce D. Fulton, Zhigang Chen, and Feng Ni

Biomolecular NMR Laboratory, Biotechnology Research Institute, National Research Council of Canada, Montréal, Québec H4P 2R2, Canada

Received March 11, 1998; Revised Manuscript Received May 5, 1998

ABSTRACT: Substrate hydrolysis by human cytomegalovirus (HCMV) protease is essential to viral capsid assembly. The interaction of HCMV protease and the N-terminal cleavage products of the hydrolysis of R- and M-site oligopeptide substrate mimics (**R** and **M**, respectively, which span the P9−P1 positions) was studied by NMR methods. Protease-induced differential line broadening indicated that ligand binding is mediated by the P4−P1 amino acid residues of the peptides. A well-defined extended conformation of **R** from P1 through P4 when complexed to HCMV protease was evidenced by numerous transferred nuclear Overhauser effect (NOE) correlations for the peptide upon addition of the enzyme. NOE cross-peaks between the P4 and P5 side chains placing these two groups in proximity indicated a deviation from the extended conformation starting at P5. Similar studies carried out for the **M** peptide also indicated an extended peptide structure very similar to that of **R**, although the conformation of the P5 glycine could not be established. No obvious variation in structure between bound **R** and **M** (notably at P4, where the tyrosine of the R-site has been suggested to play a key role in ligand binding) could be discerned that might explain the observed differences in processing rates between R- and M-sequences. Kinetic studies, utilizing R- and M-site peptide substrates for which the P5 and P4 residues were separately exchanged, revealed that these positions had essentially no influence on the specificity constants (k_{cat}/K_M). In sharp contrast, substitution of the P2 residue of an M-site peptide changed its specificity constant to that of an R-site peptide substrate, and vice versa.

The human cytomegalovirus (HCMV)[1] is a highly prevalent pathogen that poses a serious risk to immunocompromised individuals, notably AIDS patients, organ transplant recipients and neonates who acquire the infection congenitally (*1*, *2*). Typical of members of the Herpesvirus family, HCMV encodes a unique protease involved in capsid assembly whose activity is essential to the production of infectious virions (*3*−*6*). The enzyme is responsible, late in the viral cycle, for the processing of the assembly protein whose function is analogous to that of the "scaffolding" protein of bacteriophages (*7*). In the case of HCMV's close homologue HSV-1, failure to process the assembly protein results in the accumulation of aberrant, noninfectious capsids (*5*).

The full-length HCMV protease (AC_{pra}) contains 708 amino acids encoded by the UL80 gene, which is coterminal with the UL80.5 open reading frame (ORF) (*3*). The UL80.5 ORF codes for the assembly protein precursor (pAP) and is in frame with the 373 carboxyl-terminal amino acids of the protease. As a result, the enzyme can process its own C-terminus at a site identical to that of its substrate (maturation or M-site). The protease also undergoes self-processing at a release (R-) site near its amino terminus. This cleavage liberates the 256 amino acid catalytic domain, which is a member of the serine protease family; however, it possesses a number of unique features. X-ray crystallographic analysis (*8*−*11*) has shown it to possess a unique protein fold and an unusual catalytic triad in which the third member is a histidine. Also setting it apart from classical serine proteases is its existence as a dimer, which is believed

[†] This work was supported, in part, by the National Research Council of Canada (NRCC Publication 41429).

[‡] The structure described in this paper has been deposited in the Brookhaven Protein Data Bank under filename 1BFZ.

* Address correspondence to this author at Department of Chemistry, Bio-Méga Research Division, Boehringer Ingelheim (Canada) Ltd., 2100 Cunard St., Laval, Québec H7S 2G5, Canada. Telephone (514) 682-4640; Fax (514) 682-8434.

[1] Abbreviations: CMV, cytomegalovirus; HCMV, human cytomegalovirus; HSV, herpes simplex virus; AP, assembly protein; AC_{pra}, full-length human cytomegalovirus protease precursor; pAP, assembly protein precursor; HPLC, high-performance liquid chromatography; EDTA, ethylenediaminetetraacetic acid; TSP, 3-(trimethylsilyl)propionic acid; TCEP, tris(2-carboxyethyl)phosphine; DMSO, dimethyl sulfoxide; DTT, dithiothreitol; NOE, nuclear Overhauser effect; NOESY, two-dimensional nuclear Overhauser effect spectroscopy; TOCSY, total coherence-transfer spectroscopy; NMR, nuclear magnetic resonance; TPPI, time-proportional phase incrementation; FID, free induction decay; TRNOE, transferred nuclear Overhauser effect spectroscopy.

S0006-2960(98)00555-8 CCC: $15.00
Published on Web 06/18/1998

Table 1: Amino Acid Sequences of Peptides Used in the Present Study[a]

name	P9	P8	P7	P6	P5	P4	P3	P2	P1	P1′	P2′	P3′	P4′	P5′	P6′	P7′	P8′
M	Arg	Ala	Gln	Ala	Gly	Val	Val	Asn	Ala								
R	Thr	Glu	Arg	Glu	Ser	Tyr	Val	Lys	Ala								
M−**M**′	Arg	Ala	Gln	Ala	Gly	Val	Val	Asn	Ala	Ser	Cys	Arg	Leu	Ala	Thr	Ala	Ser-NH_2
R−**R**′	Thr	Glu	Arg	Glu	Ser	Tyr	Val	Lys	Ala	Ser	Val	Ser	Pro	Glu	Ala	Ala	Cys-NH_2
M−**R**′	Arg	Ala	Gln	Ala	Gly	Val	Val	Asn	Ala	Ser	Val	Ser	Pro	Glu	Ala	Ala	Cys-NH_2
R−**M**′	Thr	Glu	Arg	Glu	Ser	Tyr	Val	Lys	Ala	Ser	Cys	Arg	Leu	Ala	Thr	Ala	Ser-NH_2
M(G → S)	Arg	Ala	Gln	Ala	Ser	Val	Val	Asn	Ala	Ser	Cys	Arg	Leu	Ala	Thr	Ala	Ser-NH_2
M(V → Y)	Arg	Ala	Gln	Ala	Gly	Tyr	Val	Asn	Ala	Ser	Cys	Arg	Leu	Ala	Thr	Ala	Ser-NH_2
M(N → K)	Arg	Ala	Gln	Ala	Gly	Val	Val	Lys	Ala	Ser	Cys	Arg	Leu	Ala	Thr	Ala	Ser-NH_2
R(S → G)	Thr	Glu	Arg	Glu	Gly	Tyr	Val	Lys	Ala	Ser	Val	Ser	Pro	Glu	Ala	Ala	Cys-NH_2
R(Y → V)	Thr	Glu	Arg	Glu	Ser	Val	Val	Lys	Ala	Ser	Val	Ser	Pro	Glu	Ala	Ala	Cys-NH_2
R(K → N)	Thr	Glu	Arg	Glu	Ser	Tyr	Val	Asn	Ala	Ser	Val	Ser	Pro	Glu	Ala	Ala	Cys-NH_2

[a] Unnatural substitutions are underlined.

to be the sole active species (*12*, *13*). Finally, our spectroscopic studies (*14*) have demonstrated that the binding of substrate-based competitive inhibitors results in a conformational change in the enzyme and that catalysis by HCMV protease can be best described in terms of an "induced fit" model.

In the present work, we provide a detailed account of NMR investigations focusing on the interaction of HCMV protease with the N-terminal cleavage products of R- and M-site oligopeptide substrate mimics (denoted **R** and **M**; see Table 1 for the amino acid sequences of all peptides employed in the present work). In the case of the R-site sequence, a bound conformation obtained through transferred NOEs and molecular modeling is described, which represents the first detailed 3D structure of an HCMV protease-bound peptide, which will be of utility in the design of inhibitors of the enzyme. Kinetic data are described that underline the central importance of the amino acid residues N-terminal to the scissile bond [P-side, according to the nomenclature of Schechter and Berger (*15*)]. Finally, a key focus of the present investigation was the identification of structural elements within the R- and M-site recognition sequences that might account for the more rapid hydrolysis of the latter. No significant differences were apparent between the bound structures of **R** and **M** (from P1 to P4), and reexamination of the cleavage of substituted oligopeptide substrates point to the P2 side chain, and not P4 or P5, playing the principal role in the observed variation in cleavage rates.

MATERIALS AND METHODS

Enzymes and Substrates. Kinetic measurements were carried out with wild-type HCMV protease (*18*). Peptide substrates as well as their cleavage products were synthesized by solid phase established protocols (*16*) or were obtained from Advanced Chemtech or Multiple Peptide System. In all cases, the purity of the peptides was greater than 95% as determined by HPLC. NMR experiments employed the HCMV protease mutant Ala143Gln to overcome the problem of autoproteolysis (*17*). Full details of the preparation and the purification of recombinant enzyme to >99% purity have been described elsewhere (*14*, *18*).

Kinetic Studies. HCMV protease activity was determined by monitoring the cleavage of 17-mer peptides corresponding to the natural P9−P8′ sequences of the maturation (M) and release (R) sites as well as that of chimeric substrates incorporating the N-terminal (P-side) end of a site with the C-terminal end (P′-side) of a different site. HCMV protease (500 nM) was incubated with 25 μM substrate in a buffer composed of 50 mM Tris-HCl, pH 8, 50 mM NaCl, 0.1 mM EDTA, 0.5 M Na_2SO_4, 1 mM TCEP, 5% (v/v) DMSO, and 0.05% (w/v) casein in a total volume of 600 μL at 30 °C. At regular time intervals corresponding to less than 30% conversion, 50 μL aliquots were diluted to 150 μL with 1% trifluoroacetic acid to stop the reaction and the quenched mixtures were analyzed by reversed-phase HPLC (C-8, PE XPRESS 3 × 3CR, 3.3 × 0.6 mm; Perkin-Elmer, Norwalk, CT). The substrate and product fragments were eluted with gradients of acetonitrile in aqueous 3 mM SDS and 0.05% (v/v) H_3PO_4. A typical gradient consisted of a 25−38% (v/v) acetonitrile elution over 11 min at a flow rate of 4 mL/min. The extent of conversion was determined by comparing the peak area of either the N- or C-terminal fragment at the various quenching times to a corresponding standard curve prepared under identical buffer conditions. The concentration of enzyme was expressed in terms of total monomer concentration as determined by the Bradford method (*19*). The specificity constant (k_{cat}/K_M) was obtained by dividing the initial slope of a graph of product versus time by both the initial enzyme and substrate concentrations. This procedure is consistent with the use of 25 μM substrate, which is well below the K_M values reported for such peptides (*20*).

NMR Experiments. Two identical samples were initially prepared for each 1D NMR experiment. Sample tubes (5 mm) containing 2 mM peptide were prepared by adding concentrated solutions of either **R** or **M** in DMSO-d_6 to an aqueous buffer composed of 50 mM Tris-d_{11}, 0.5 M Na_2SO_4, 50 mM NaCl, 1 mM EDTA, and 5 mM DTT-d_{10} in 10% D_2O spiked with TSP-2,2,3,3-d_4. The final pH values of the solutions were adjusted to 7 and buffer was added to a final volume of 600 μL.

To one of the above samples was added a concentrated stock solution of HCMV protease (20 mg/mL) in a buffer identical to that employed above, however, containing EDTA-d_{16} and no TSP. Aliquots of enzyme solution were added until protease/peptide ratios of 1:15 and 1:7 were reached. The EDTA and TSP signals were used to normalize resonance intensities to identify resonance perturbations induced by the addition of enzyme (i.e., differential line broadening).

One-dimensional spectra were acquired on a Bruker AMX400 spectrometer at 27 °C for each incremental addition of the enzyme. Suppression of the solvent signal was

achieved by the use of presaturation or the WATERGATE method (*21*). Two-dimensional NOESY and TOCSY experiments were carried out on Bruker AMX500, DRX500, or DMX600 instruments equipped with pulse-field gradient accessories. Phase-sensitive spectra were acquired by the TPPI method (*22*) in conjunction with standard NOESY (*23*) and TOCSY (*24*) phase cycles. For some experiments, the initial delay of the evolution period was set to exactly one dwell period to minimize baseline distortion along *F*1 (*25*). Water suppression was achieved by inserting a 3−9−19 WATERGATE module prior to data acquisition (*21*, *26*). NOESY experiments were recorded with a water-selective flip-back pulse prior to the readout pulse to maintain the water magnetization along the positive *z*-axis during the acquisition period and relaxation delay (*27*). The MLEV-17 mixing scheme (*24*) and a mixing time of 70 ms were used for all TOCSY experiments. All 2D NMR data were acquired at 15 °C while certain spectra were also obtained at 30 °C.

Two-dimensional data sets were acquired with 2048 points in t_2 and 400 points in t_1. 128 scans were averaged for NOESY FIDs and 64 scans for TOCSY FIDs. The data were processed with Bruker XWinNMR software. Data sets were zero-fitted to yield 2048 by 1024 real points after transformation with a phase-shifted sinebell window function.

Computational Methods. The structure of the peptide **R** was modeled using Discover 95.0 and the CFF95 force field (Molecular Simulations Inc., 9685 Scranton Rd., San Diego, CA 92121-3752). All calculations were performed without nonbonded or Coulombic cutoffs and with a dielectric constant of 1.0. Experimentally derived distance restraints were generated from the NOE data by a method similar to that of Baleja et al. (*28*). NOESY spectra were acquired with a range of mixing times (50−350 ms) at 15 and 30 °C to help identify spin-diffusion effects (*25*, *29*). The restraints were applied as strong (1.8−2.7 Å), medium (1.8−3.5 Å), or weak (1.8−5.0 Å) flat-bottomed potentials. A single, high-temperature unrestrained dynamics run was performed at 1000 K with a time step of 1 fs, with 50 structures collected at 1.5 ps intervals to generate a starting set of conformations. Each structure was cooled and minimized by use of the following simulated annealing protocol. The temperature was lowered to 500 K at a rate of 25 K/ps where strong restraints were applied, followed by additional cooling to 250 K (12.5 K/ps). The remaining restraints were added and cooling to 50 K (6.75 K/ps) was performed, followed by restrained minimization to a final gradient of 0.01 kcal/mol·Å. A total of 32 lowest-energy structures were isolated and a representative structure consistent with the NMR data was selected.

RESULTS AND DISCUSSION

The overall goal of the present work was to acquire a clear understanding of the structural elements of the substrate that are required for complexation with HCMV protease. Both NMR and kinetic methods were employed to obtain a concise picture of which residues play a role in substrate recognition by the enzyme, as well as to analyze the overall conformational features of the residues critical to binding of the ligand. Also of interest was the investigation of any differences in the binding modes of the M and R sequences in order to understand the structural basis of the differing processing rates between these two sites.

NMR studies involving full processing site sequences would undoubtedly represent the most direct approach to obtaining information concerning substrate binding (*30*). Although the proton NMR spectrum of a P9−P8′ R-site substrate mimic **R**−**R′** could be obtained in the presence of HCMV protease, which indeed exhibited changes in certain proton resonances as compared to that of the free peptide, the rapid enzymatic cleavage to product fragments and the emergence of new signals precluded any detailed NMR studies of the bound and intact processing site sequences. This did, however, allow for the monitoring of the cleavage of **R**−**R′** to its completion. Comparison of the resonances of the N-terminal cleavage product **R** in the final reaction mixture with those of another NMR sample containing only **R** clearly revealed resonance perturbations in the former as a result of rapid exchange between free and protease-bound states of the peptide and indicating that transferred NOE methods could be applied to obtain a bound conformation of the product fragment (data not shown).

The decision to focus subsequent structural studies on the N-terminal cleavage products **R** and **M** was based, in addition, on both existing enzymological data and our own kinetic studies (see below), which indicate a more important role for the P-side residues over those of the P′ sequence in substrate binding by HCMV protease, in accord with the behavior of serine proteases in general (*31*). We have observed that amino acid substitutions of P′ residues have a much less pronounced effect on oligopeptide substrate hydrolysis rates than those of P-side residues (data not shown), as has also been described in the literature (*32*). The finding that the P4−P1′ M-site core alone is capable of competitively inhibiting catalysis with binding only 5-fold less than a P4−P4′ substrate (*33*) also supports the presumption that the structural elements of the substrate N-terminal to the scissile bond are crucial to its complexation by the enzyme.

Determination of P Residues Involved in Substrate Binding by Differential Line Broadening Experiments. Our initial NMR investigations focused on confirming that the P9−P1 N-terminal products **R** and **M** were indeed binding in a specific fashion to the enzyme and determining which residues were involved in the interaction. Figure 1A presents a portion of the 1D proton spectrum of **R** and shows the signals of the P1-alanine and P9-threonine methyl doublets in the presence and absence of the enzyme. In the case of the spectrum acquired in the presence of HCMV protease (7-fold excess of peptide over protease), differential line broadening was evident, the P1 signal being clearly altered compared to the resonance in the absence of protease, whereas no significant change was seen in the P9 methyl signal. A lesser effect, as one would anticipate in the case of specific binding of the peptide, was observed for a 15-fold excess of the ligand over the enzyme.

To establish that complexation was indeed at the active site of HCMV protease, a number of competition experiments were carried out. In Figure 1B, the protease-induced line broadening of the P1 signal of **R** is again presented. Upon the addition of a potent, competitive inhibitor of the enzyme, the peptidyl pentafluoroethyl ketone PFEK [*N*-*tert*-butylacetyl-L-*tert*-butylglycyl-L-N^{γ},N^{γ}-dimethylasparagyl-L-ala-

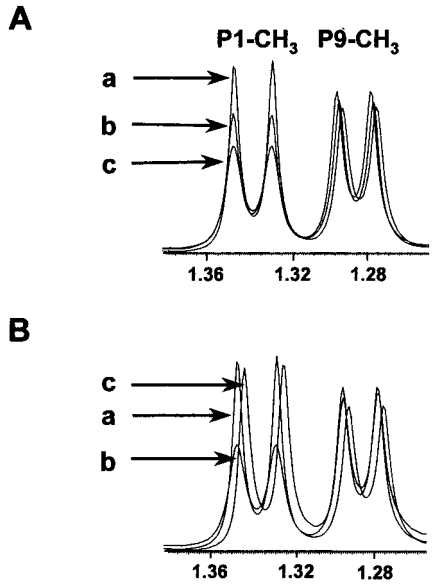

FIGURE 1: Methyl region of the NMR spectrum of **R** showing the P1 and P9 side chain doublets. (A) (a) 2 mM **R** alone; (b) **R** to HCMV protease ratio of 15:1; and (c) **R** to HCMV protease ratio of 7:1. The P1 methyl signals have been aligned to show the concentration-dependent differential line broadening. (B) Changes in the signals of (a) 2 mM **R** alone and (b) upon the addition of HCMV protease to a 7:1 ratio of **R** to protease. (c) Signals after the subsequent addition of the potent competitive inhibitor **PFEK** to a 7:1:2 ratio of **R**/protease/**PFEK** demonstrating the displacement of **R** from the active site of the enzyme. For the sake of clarity, the P1 methyl signals have been skewed slightly.

nyl pentafluoroethyl ketone, $IC_{50} = 0.1\ \mu M$; see Ogilvie et al. (*34*)], the P1 methyl signal was fully restored to its original uncomplexed form owing to the inability of **R** to enter the fully blocked active site. Our previous NMR studies (*14*) have clearly shown that PFEK is complexed by HCMV protease at the active site where it forms a stable hemiketal adduct with the catalytic serine.

A more thorough analysis of the enzyme-induced changes in the peptide signals allowed us to extract more detailed information concerning the factors governing ligand binding to HCMV protease. Changes in the observed peak shape and intensity due to averaging of the free and bound signals, which may differ in both chemical shift and line shape, are indicative of interaction between the macromolecule and the specific proton(s) in question. A systematic comparison of corresponding resonances in the free and protease-bound peptide spectra was carried out whenever possible to determine which residues presented protein-induced line broadening. The results are tabulated in Figure 2 and indicate that for both **R** and **M** nonamers, it is within the P4−P1 region that changes in the signals are observed and binding is mediated. Little interaction with the protease appeared to occur beyond P5 (as also demonstrated in Figure 1).

While kinetic studies have inferred the same, the present NMR line-broadening results represent the first direct physical evidence that it is the P4−P1 core which is, in very large part, responsible for substrate recognition by HCMV protease. Kinetic studies involving M-site oligopeptide mimics have all demonstrated little decrease in cleavage efficiency with N-terminal truncation of oligopeptide substrates up to the P4 position, followed by a substantial loss of activity

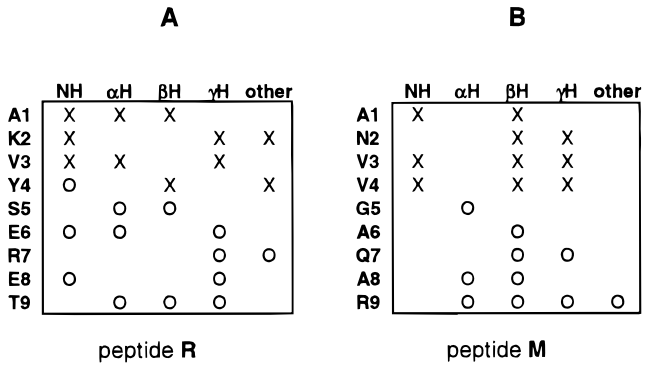

FIGURE 2: Tabulation of line-broadening effects observed for (A) **R** and (B) **M** in the presence of 0.28 mM HCMV protease. X indicates the observation of line broadening, whereas O denotes the absence of any discernible changes in the resonance.

upon removal of the P4 valine (*32*, *33*, *35*). Consistent with these observations are data from our medicinal chemistry efforts involving peptidyl-activated carbonyl inhibitors of HCMV protease, which show a sharp rise in IC_{50} value upon removal of the P4 residue (*34*). Carboxyl-terminal truncation of substrates bearing the minimal P4−P1 core has demonstrated P4−P5′ or P4−P4′ to be the minimal sequence for "efficient" cleavage, although hydrolysis has been observed for a sequence as short as P4−P3′ (*32*). In the case of R-site mimics, it has been reported that N-terminal truncation has little effect on the hydrolysis rate until the P5 serine is removed (*35*).

In the case of the M-site, the above kinetic studies are fully consistent with our differential line-broadening observations for which all analyzable resonances of the P4−P1 residues exhibited protease-induced changes in the signals. The data for the R-site mimic are similar, the P1 through P4 resonances being altered in the presence of enzyme and those beyond the P4 residue not presenting any changes. The single exception is the P4-Tyr NH signal, which remains unaffected, indicating that the environment of the P4−P5 amide may differ somewhat from that of the corresponding linkage in the M-site peptide. Another fact to be noted is that whereas the present line-broadening data suggest that the R-site P5 Ser is not in close proximity to the protein, the presence of this residue appears to be important to substrate hydrolysis on the basis of the above-cited truncation study (*35*).

*Determination of the Bound Structures of Peptides **R** and **M** by Transferred NOE Methods.* Having established the region of the substrate that plays the most important role in its complexation by the protease, we then focused our efforts on determining the conformational properties of the key P4−P1 sequences of **R** and **M**. To assist signal assignment, TOCSY spectra of the free nonamers were first obtained. The amide/aromatic region of the spectrum of **R** is presented in Figure 3A and, typical for a molecule of its size, presents intense TOCSY signals for which the expected intraresidue correlations could be identified. Only the P8 Glu signals were weak, but they nonetheless allowed for unambiguous assignment. The NOESY spectrum of the same sample (Figure 3B) was also obtained and consisted of only a small number of weak signals, primarily the intraresidue NH−αH cross-peaks typically observed for a short peptide of this length.

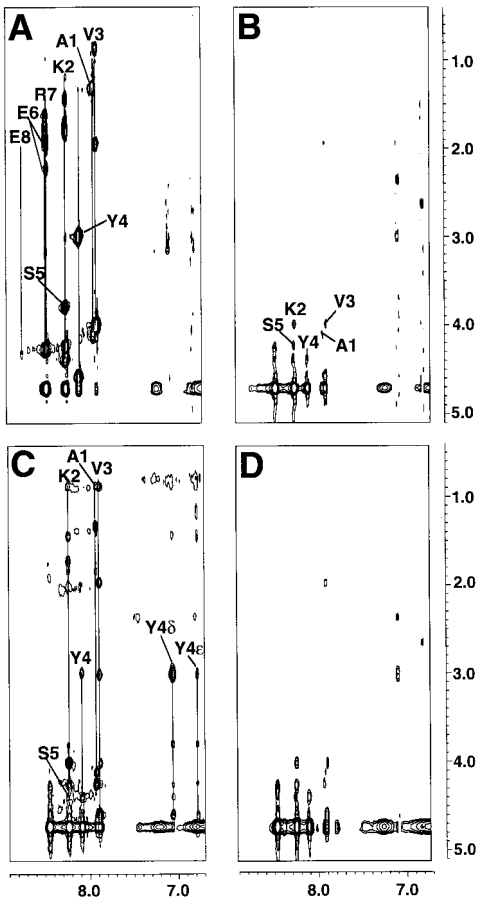

FIGURE 3: Amide/aromatic to aliphatic region of the two-dimensional NMR spectra of 2 mM **R**. Amino acid residues are denoted according to P-residue numbering. (A) TOCSY spectrum of **R** alone, showing intraresidue NH correlations. (B) NOESY spectrum of 2 mM **R** alone, presenting a small number of weak NH−C$^{\alpha}$H cross-peaks. (C) NOESY spectrum of 2 mM **R** following the addition of HCMV protease (7:1, respectively) resulting in numerous NH−aliphatic cross-peaks absent in panel B. (D) NOESY spectrum of **R** in the presence of HCMV protease after the addition of **PFEK** (in a 7:1:2 ratio). The NOESY spectra were all acquired under identical conditions (see Materials and Methods).

The NOESY spectrum of a large excess of **R** was then acquired in the presence of HCMV protease. As is evident in Figure 3C, many new cross-peaks were visible, principally correlations between intraresidue protons. In addition, a number of interresidue cross-peaks appeared and those already present in the spectrum of the free peptide dramatically increased in intensity. These results indicate a well-defined and rapidly reversible binding of **R** to the enzyme. Finally, the strong competitive inhibitor PFEK was added to the sample at a concentration equal to that of the protease and the NOESY spectrum reacquired (Figure 3D). The resulting disappearance of the new cross-peaks and the restoration of the spectrum to that of the free peptide is indicative of the displacement of **R** from the active site by the potent peptidyl-activated carbonyl inhibitor. The analogous series of 2D experiments were also carried out for **M**, which afforded very similar results (data not shown).

*Structure of Peptide **R***. The intensities of transferred NOE cross-peaks provide information concerning the enzyme-bound conformations of the peptides since they are proportional to the interproton distances separating hydrogen atoms of the complexed ligands (*25*). Figure 4A presents the NH−

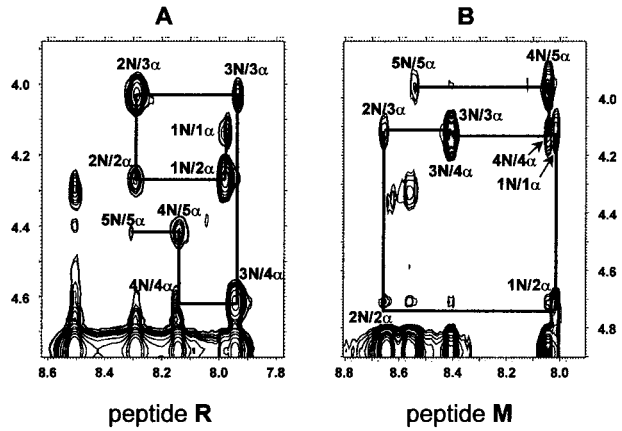

FIGURE 4: Sequential backbone transferred NOE connectivities in the NH−C$^{\alpha}$H region of the NOESY spectra of (A) **R** and (B) **M** in the presence of HCMV protease. Alternating NH(i)−C$^{\alpha}$H(*i*) and NH(1)−C$^{\alpha}$H(i + 1) cross-peaks are labeled according to the P-residue number.

αH or "fingerprint" region of the NOESY spectrum of **R** in the presence of HCMV protease, showing the sequential transferred NOE connectivities. The backbone sequence may be traced from the P1 alanine to the P5 serine residues. From examination of the 1D spectrum of **R**, and consistent with its cross-peak forms, it was clear that the intensities of the Ser5 NH signals were diminished due to solvent exchange in the free state and could not be interpreted in a meaningful fashion. No interresidue correlations were observed between P6 and P7, and the P8 and P9 residues did not give rise to any transferred NOE peaks whatsoever. This suggests that the N-terminal half of **R** does not possess a defined conformation in either the free or protease-bound states and, consistent with the line-broadening data, is not likely implicated in complexation by the protease.

The clear pattern of alternating interresidue [C$^{\alpha}$H(*i*)−NH(i + 1)] cross-peaks of strong intensity is characteristic of an extended peptide conformation (*36*) from P1 to P4. This is corroborated by the absence of any NH(*i*)−NH(i + 1) NOESY peaks. The pattern indicative of an extended chain is broken at P5, where the NOE between the Tyr4 NH and Ser5 αH atoms is much less intense than expected for such a conformation. Furthermore, cross-peaks between the Ser5 methylene and Tyr4 aromatic protons (Figure 5A) place the two side chains in proximity, indicating a bend in the structure of the peptide.

Owing to the presence of many analyzable cross-peaks, some of which are presented in Figure 5A, an NMR-derived structure of enzyme-bound **R** was obtained through molecular modeling. The NOESY cross-peak volumes were scaled and converted to interproton distance restraints (*28*) using the P1 Ala-NH to P2 Lys-αH cross-peak to correlate the volumes with distances. Figure 6A depicts 32 low-energy, transferred NOE-derived structures generated by restrained simulated annealing, presented in a superimposed fashion. The extended peptide conformation is clearly evident from P1 through P4 for all of the structures, which show only a small deviation along the backbone chain within this sequence. The tyrosine side chain and Ser5 residue exhibited a much greater degree of variability owing to the smaller number of analyzable NOE correlations for this region of the peptide. It is clear, nonetheless, that the peptide chain is kinked at P4−P5 with the two side chains in proximity.

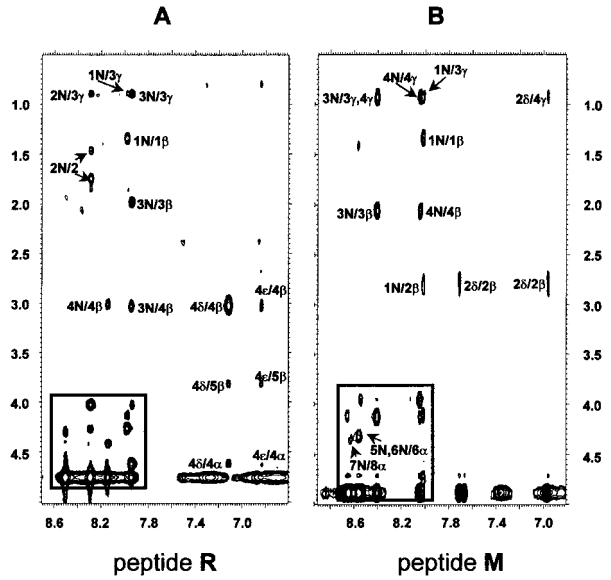

FIGURE 5: Selected regions of the transferred NOE spectra of **R** and **M** complexed to HCMV protease showing amide/aromatic to aliphatic correlations. The regions of the 2D spectra presented in Figure 4 are outlined in boldface type.

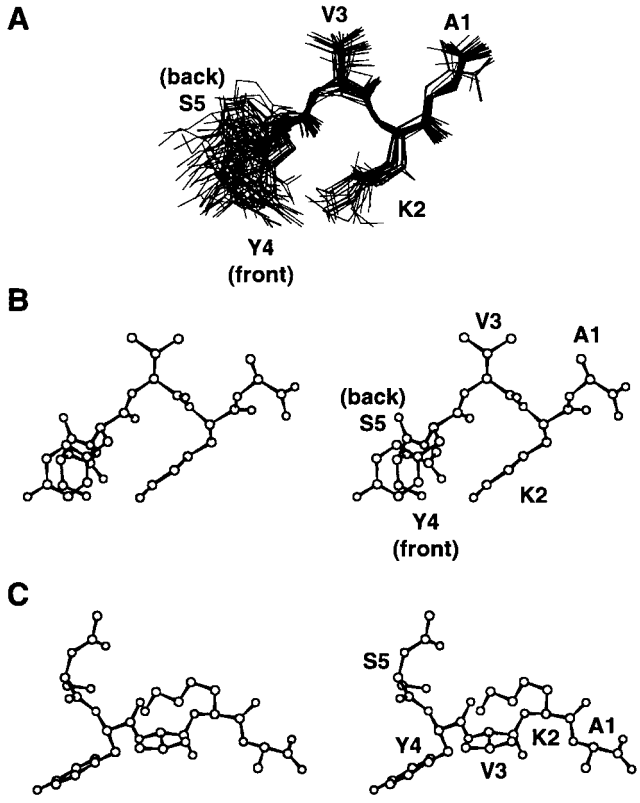

FIGURE 6: Conformation of the P1−P5 sequence of **R** when bound to HCMV protease. (A) View of 32 overlapped structures determined by restrained simulated annealing. (B) A representative conformation most consistent with the NMR data showing the P1−P4 sequence in an extended backbone conformation and the P4−P5 sequence in a turn conformation. (C) The same structure rotated horizontally approximately 90° with respect to panel B.

Panels B and C of Figure 6 present stereoviews of a structure selected among those generated as best reflecting the NMR data, which we put forth as the NMR-derived bound conformation of **R** when complexed to HCMV protease.

*Structure of Peptide **M***. The NH−αH region of the NOESY plot of **M** in the presence of HCMV protease is shown in Figure 4B and also presents many enzyme-induced cross-peaks. Two facts preclude as straightforward an analysis as in the case of **R**: (a) the reduced intensity of the P2 Asn backbone amide resonance due to solvent exchange in the free state and (b) the unfortuitous coincidence of the P3 and P4 valine α-proton chemical shifts, which rendered uninterpretable the key correlations to neighboring amide protons. As in the case of **R**, the intensity of the P5 NH was reduced due to solvent exchange in the free state and very few correlations beyond P5 were noted. Despite these limitations, however, a fairly clear conformational picture could be extracted from the NOESY data. The P1 and P2 residues are extended as evidenced by the weak and strong cross-peaks between the P1 Ala-NH and the P1 and P2 α-protons, respectively. The weak intraresidue NH−αH correlation within Val4 is also consistent with an extended conformation. A key cross-peak is that observed between one of the P2 Asn side chain amide protons and a P4 Val methyl group, which places the two side chains within a distance only possible for an extended backbone chain. This is also supported by the absence of any NH(i)−NH(i + 1) NOESY peaks. Although the uninterpretable nature and/or overlap of certain key correlations made impossible any structure calculations, a systematic analysis of all analyzable NOESY signals and the absence of amide−amide cross-peaks leads us to conclude that the peptide **M** as well assumes an extended peptide conformation along P1 through P4. This is corroborated by related NMR investigations carried out for a tetrapeptidyl methyl ketone probe closely related to the P4−P1 M-site sequence for which transferred NOE and molecular modeling studies provided an HCMV protease-bound structure in an extended peptide conformation (unpublished results). Furthermore, this structure is very similar to that derived for the R-site peptide in the present work. Thus, the present results indicate that both **R** and **M** are complexed by HCMV protease in very similar extended peptide conformations within the key P4−P1 sequences.

Because HCMV protease undergoes a structural transition upon the binding of peptidyl ligands (*14*), the question arises whether the complexed peptide products can also exist in more than one bound conformation. We believe that, throughout the binding process and the structural adjustment of the enzyme, the conformation of the peptide remains the same. The consistency among the NOE distance constraints for structural calculations indicate that any alterations in the conformations of bound **R** and **M**, if any, must be minor. In cases where there is clear evidence of mixed bound conformations, the situation may be handled within a theoretical framework where conformational changes can be accounted for in the interpretation of the TRNOE data for enzyme−ligand complexes (*29*). A recent example of such an investigation of a system involving two-state binding, namely, the complexation of glutathione by glutathione transferase, has been described (*37*).

Differences in M- and R-Site Processing Rates. Both the M and R cleavage sites are highly conserved among herpesvirus protease homologues (*3*, and references therein), consisting of a fairly specific consensus sequence of (V/I/L)-X-A^{i}(S/A). In the case of the R-site, the P4 Tyr residue is absolutely conserved. For HCMV protease, the consensus narrows to (Y/V)-V-(N/K)-A^{i}S. The more rapid processing of M-site over R-site sequences is a well-established fact

Table 2: Specificity Constants of Processing Site Mimics and Chimeric Substrates[a]

	M-	(factor)	**R-**
-M′	657	(10)	66
(factor)	(2.6)		(1.6)
-R′	256	(6.1)	42

[a] k_{cat}/K_M values given in molar^{-1} second^{-1}; see Table 1 for amino acid sequences of substrates.

for the in vitro cleavage of peptidic substrates as well as for the processing of AC_{pra} in cellular systems. In the latter case, it has been demonstrated that the ordered cleavage is indeed a kinetic effect and not due to prerequisite M-site processing prior to R-site hydrolysis (*38*, *39*). In view of the biological relevance of this difference in processing rate, which is no doubt of importance to the polyvalent function of HCMV protease in the capsid assembly process, we focused our subsequent efforts on discerning any appreciable differences between the structures of bound **R** and **M** that might constitute the basis for the observed differences in cleavage rates. Although studies involving proteinaceous substrates may obviously prove more relevant to the in vivo processes, we assume that the present peptidic substrates represent a valid model system, notably in light of the observed difference in the specificity constants for the enzymatic hydrolysis of **M**−**M′** and **R**−**R′**.

The values of k_{cat}/K_M for **R**−**R′** and **M**−**M′** reported in Table 2 are comparable to those previously provided in the literature (*32*, *35*, *40*, *41*). Furthermore, the present data reveals that the M-site sequence is cleaved 16 times more rapidly than the R-site mimic, which is also consistent with kinetic measurements reporting similar relative hydrolysis rates (*35*, *40*). These latter studies have also revealed that the differing cleavage rates do not stem from a variation in the respective K_M values of the peptides but are a result of a higher turnover rate (k_{cat}) in the case of M-site peptide cleavage. Investigations of substituted oligopeptide substrates have provided some information concerning the structural requirements for M-site sequence processing, notably the importance of large hydrophobic residues at P3 and P4 (*32*). Replacement of the P2 Asn by either Asp, Gln, or Glu resulted in a 10-fold decrease in specificity constant. It is noteworthy that P2 substitution with lysine resulted in a substantial decrease in cleavage rate. No data concerning substituted R-site peptide substrates have been reported.

Chimeric Substrates. The first series of kinetic studies employing substrates of unnatural amino acid sequence involved the measurement of the k_{cat}/K_M values for the hydrolysis of chimeric substrates in which P and P′ sequences are interchanged, the values for which are provided in Table 2. When holding the P-side constant (columns), substituting an **-M′** sequence with an **-R′** sequence results in a modest, roughly 2-fold, decrease in the specificity constants. Conversely, replacement of an **M** sequence by the P-side amino acids of an R-site has a much greater effect on the hydrolytic rate, which decreases 10-fold in going from **M**−**M′** to **R**−**M′**.

These results are important in two respects. Considered in a general fashion, they are consistent with the view that the structure of the P portion of a substrate has a markedly more consequential effect on binding by the enzyme than do the P′ residues. More specifically, the data demonstrate the much more important role of the P sequence in conferring a higher k_{cat}/K_M value to the hydrolysis of the M-site oligopeptide **M**−**M′** over that of its R-site counterpart.

*Comparison of Protease-Bound **R** and **M**.* A number of reasons may account for the more rapid cleavage of the M-site sequence over that of the R-site. Most obvious may be that the overall modes of substrate binding, albeit comparable in strength of complexation, are appreciably different between the **M**−**M′** and **R**−**R′** substrates. This is clearly not the case, as evidenced by the present NMR investigations, which clearly show that both of the peptides **R** and **M** are complexed by the protease in extended conformations of overall similarity, at least within the key P4−P1 region. To help underline this, the intensities of the corresponding NOESY cross-peaks which were well resolved for both protease-bound **R** and **M**, were tabulated (Table 3) to allow for comparison of the bound conformations of the two peptides. Despite some variations in NOE intensities, the apparent interproton distances derived indicate a close structural similarity between the two bound peptides.

Alternatively, the role of the P4 tyrosine of the R-site, strictly conserved among herpesviruses, has been the focus of much attention. In the case of in vivo studies involving HSV protease, P4 substitutions with amino acids active in the case of M-site cleavage were not tolerated, arguing for a critical role of the P4 Tyr as an element of the substrate and revealing a specificity difference between the two sites (*42*). It has been hypothesized that at least part of this

Table 3: Comparison of Cross-Peak Volumes and Interproton Distances Derived from the NOESY Spectra of HCMV-Bound **R** and **M** Peptides[a]

R peptide			**M** peptide		
cross-peak	volume	apparent distance (Å)	cross-peak	volume	apparent distance (Å)
Ala1-NH/Lys2-αH	15 400	2.3	Ala1-NH/Asn2-αH	15 400	2.3
Ala1-NH/Ala1-αH	1900	3.2	Ala1-NH/Ala1-αH	3100	3.0
Ala1-NH/Ala1-βCH_3	4200	2.9	Ala1-NH/Ala1-βCH_3	4500	2.8
Ala1-NH/Val3-γCH_3	900	3.7	Ala1-NH/Val3-γCH_3	1300	3.5
Ala1-NH/Lys2-βCH_2	400	4.2	Ala1-NH/Asn2-βCH_2	1100	3.6
Val3-NH/Val3-βCH	3600	2.9	Val3-NH/Val3-βCH	7500	2.6
Val3-NH/Val3-γCH_3	1800	3.3	Val3-NH/Val3-γCH_3	4400	2.9
Tyr4-NH/Tyr4-αCH	1200	3.5	Val4-NH/Val4-αCH	2250	3.2
Tyr4-NH/Tyr4-βCH	1800	3.3	Val4-NH/Val4-βCH	4300	2.9
Tyr4-NH/Ser5-αCH	2500	3.1	Val4-NH/Gly5-αCH_2	6800	2.6

[a] NOESY spectra were acquired at 15 °C with a mixing time of 150 ms. Values are normalized to the Ala1-NH/Lys2-αH cross-peak of the **R** peptide.

Table 4: Specificity Constants of Processing Site Mimics Bearing P5, P4, or P2 Substitutions[a]

peptide	position of substitution	k_{cat}/K_M (M^{-1} s^{-1})
M−**M′**		657
M(G → S)	P5	875
M(V → Y)	P4	952
R−**R′**		42
R(S → G)	P5	45
R(Y → V)	P4	37
M(N → K)	P2	58
R(K → N)	P2	282

[a] See Table 1 for amino acid sequences of substrates.

residue's necessary presence in the case of HCMV may be in rendering R-sites less prone to processing (*3*, *40*), likely by altering the overall presentation of the key P4−P1 recognition sequence by macromolecular substrates. It is, however, important to retain the fact that the varying specificities of the M- and R-sites are observed for oligopeptide substrates which are primarily unstructured in solution, and that such a role for the P4 tyrosine, at least in these cases, does not involve its participation in stabilizing a particular secondary structural feature present in the macromolecular substrates.

To address the issue of a possible role for the R-site P4 residue, we focused on identifying possible structural differences between the two peptides in the P4−P5 region. Whereas the turn at this location depicted in Figure 6 for the **R** peptide could be derived from the transferred NOE data, as straightforward an analysis of the conformation of the corresponding residues in **M** was not possible. This was due to the overlap of the two α-methylene proton resonances of Gly5 and the absence of a P5 side chain. However, considering the conformational flexibility associated with glycine residues, devoid of a side chain imposing steric constraints, there is nothing to indicate that **M** cannot be complexed by the enzyme in a manner entirely analogous to that described for **R**.

Cleavage Kinetics of P5, P4, and P2 Substituted M- and R-Site Sequences. Prompted by the fact that no obvious structural differences between protease-bound **R** and **M** within the key P4−P1 sequences were observed through the NMR investigations, the notion that the P4 position might play a crucial role in determining the varying hydrolytic rates between **R**−**R′** and **M**−**M′** was reevaluated from an enzymological perspective. An additional series of oligopeptide substrate mimics were prepared for which the P4 and, separately, the P5 amino acids were exchanged between the M- and R-site sequences. The decision to address the latter position as well stemmed from our observation that this residue becomes at least partially immobilized, as evidenced by differential line broadening, upon binding by the protease and that the interaction between the P4 amino acid and the enzyme might be strongly influenced by its steric interaction with the P5 residue. The specificity constants for the hydrolyses of these peptide substrates are provided in Table 4. The results clearly indicate that the P4 and P5 substitutions have very little effect on the hydrolysis rates. In the case of the M-site sequence, substitution with either a P4 tyrosine **M**(V → Y) or a P5 serine **M**(G → S) resulted in a very slight enhancement in the rates of hydrolysis. Substitution with the M-site P4 or P5 residues into the R-site substrate [**R**(Y → V) and **R**(S → G)) had no effect whatsoever on the values of k_{cat}/K_M compared to **R**−**R′**. These results are consistent with our observation that the structure of the P4 residue of tetrapeptidyl-activated carbonyl ketone inhibitors has very little effect on their potencies (*34*).

The only remaining position that differs between the recognition sequences of **R** and **M** was the P2 amino acid. Although a marked decrease in specificity constant has been reported upon substituting a P2 Lys in an M-site oligopeptide, the change did not fully account for the much lower value reported for an unmodified R-site substrate mimic (*32*). To reexamine this, both M- and R-site substrates with exchanged P2 residues [**M**(N → K) and **R**(K → N)) were synthesized. As reported in Table 4, the k_{cat}/K_M value of the modified **M** sequence drops to that of **R**−**R′**. In the case of the P2-modified R-site sequence, a marked rise in the specificity constant, albeit not fully to that of **M**−**M′**, was also observed. These results strongly suggest that it is the P2 side chain which is responsible for the differing processing rates.

CONCLUSIONS

In the present work, we provide the first bound conformation of an HCMV protease-complexed peptide corresponding to the N-terminal product of R-site cleavage. The structure, obtained through transferred NOE methods and molecular modeling, exists in an extended peptide conformation from P1 through P4, followed by a turn in the backbone chain which places the P4 and P5 side chains in proximity. Furthermore, on the basis of detailed analysis of the transferred NOE data for an equivalent P9−P1 M-site peptide, as well as through direct comparison of its NOESY data with that of the R-site peptide, we conclude that both species occupy the active site of the enzyme in a very similar conformation.

In view of the close structural similarity between the two bound peptides, and the notable absence of any discernible conformational differences in their P4 positions, a series of kinetic measurements were undertaken to clarify the role of each differing position within the key recognition sequence in determining the respective processing rates for the R and M sequences. These results clearly demonstrate that, at least in the case of oligopeptide substrates, the more rapid processing of the latter sequence stems primarily from the P2 amino acid and not to any appreciable degree from the P4 or P5 residues.

A central question addressed in this present study, i.e., why the M-site sequence is processed more rapidly than that of the R-site, may be reformulated as why does the catalytic machinery of HCMV protease act more efficiently on the former sequence when both are bound with equal strength by the enzyme? It may be that the P2 side chain lies very close to the catalytic machinery and therefore has an effect on the rate-limiting step of hydrolysis. Thus, the k_{cat} may depend on the nature of the P2 side chain. Another factor that may be of relevance is the conformational change that occurs upon binding of a peptidic ligand by the enzyme (*14*). It is plausible that while the P2 residue does not exert a signifigant effect on the stability of the encounter complex, a P2 lysine is not as effective as an asparagine in inducing the structural change within the initial Michaelis complex required for optimal catalysis.

On the other hand, since it is not known to what degree if any the conformational change limits the observed hydrolytic rate, the presumption that the K_M values clearly reflect the strength of substrate binding (i.e., that K_M and K_S values are similar) may be an oversimplification. A much more detailed understanding of the workings of this novel serine protease will be required before the precise structural basis for the processing rate differences is uncovered. Such an understanding will also, undoubtedly, aid in the rational design of inhibitors of HCMV protease and, ultimately, the development of therapeutic agents against HCMV disease.

ACKNOWLEDGMENT

We thank A. Abraham for peptide synthesis and Dr. R. Déziel for his support and helpful discussions. We are also grateful to Dr. M. T. Phan Viet, Professor J. Wuest, and S. Bilodeau for 600 MHz spectra acquired at the Université de Montréal (Département de Chimie).

REFERENCES

1. Mocarski, E. S., Jr. (1995) in *Virology 2* (Fields, B. N., Ed.) pp 2447−2492, Lippincott−Raven, Philadelphia, PA.
2. Britt, W. J., and Alford, C. A. (1995) in *Virology 2* (Fields, B. N., Ed.) pp 2493−2525, Lippincott−Raven, Philadelphia, PA.
3. Gibson, W., Welch, A. R., and Hall, M. R. T. (1994) *Perspect. Drug Discov. Des. 2*, 413−426.
4. Gao, M., Matusick-Kumar, L., Hurlburt, W., DiTusa, S. F., Newcomb, W. W., Brown, J. C., McCann, P. J., III, Deckman, I., and Colonno, R. J. (1994) *J. Virol. 68*, 3702−3712.
5. Preston, V. G., Coates, J. A. V., and Rixon, F. J. (1983) *J. Virol. 45*, 1056−1064.
6. Matusick-Kumar, L., McCann, P. J., III, Robertson, B. J., Newcomb, W. W., Brown, J. C., and Gao, M. (1995) *J. Virol. 69*, 7113−7121.
7. Casjens, S., and King, J. (1975) *Annu. Rev. Biochem. 44*, 555.
8. Tong, L., Qian, C., Massariol, M.-J., Bonneau, P. R., Cordingley, M. G., and Lagacé, L. (1996) *Nature 383*, 272−275.
9. Qiu, X., Culp, J. S., DiLella, A. G., Hellmig, B., Hoog, S. S., Janson, C. A., Smith, W. W., and Abdel-Meguid, S. S. (1996) *Nature 383*, 275−279.
10. Shieh, H.-S., Kurumbail, R. G., Stevens, A. M., Stegeman, R. A., Sturman, E. J., Pak, J. Y., Wittwer, A. J., Palmier, M. O., Wiegand, R. C., Holwerda, B. C., and Stallings, W. C. (1996) *Nature 383*, 279−282.
11. Chen, P., Tsuge, H., Almassy, R. J., Gribskov, C. L., Katoh, S., Vanderpool, D. L., Margosiak, S. A., Pinko, C., Matthews, D. A., and Kan, C.-C. (1996) *Cell 86*, 835−843.
12. Margosiak, S. A., Vanderpool, D. L., Sisson, W., Pinko, C., and Kan, C.-C. (1996) *Biochemistry 35*, 5300−5307.
13. Darke, P. L., Cole, J. L., Waxman, L., Hall, D. L., Sardana, M. K., and Kuo, L. C. (1996) *J. Biol. Chem. 271*, 7445−7449.
14. Bonneau, P. R., Grand-Maître, C., Greenwood, D. J., Lagacé, L., LaPlante, S. R., Massariol, M.-J., Ogilvie, W. W., O'Meara, J. A., and Kawai, S. H. (1997) *Biochemistry 36*, 12644−12652.
15. Schechter, J. and Berger, A. (1970) *Philos. Trans. R. Soc. London, Ser. B 257*, 249−264.
16. Fields, G. B., and Noble, R. L. (1990) *Int. J. Pept. Protein Res. 35*, 161−214.
17. Pinko, C., Margosiak, S. A., Vanderpool, D., Gutowski, J. C., Condon, B., and Kan, C.-C. (1995) *J. Biol. Chem. 270*, 23634−23640.
18. Bonneau, P. R., Plouffe, C., Pelletier, A., Wernic, D., and Poupart, M.-A. (1998) *Anal. Biochem. 255*, 59−65.
19. Bradford, M. M. (1976) *Anal. Biochem. 72*, 248−254.
20. Holwerda, B. C. (1997) *Antiviral Res. 35*, 1−21.
21. Piotto, M., Saudek, V., and Sklenar, V. (1992) *J. Biomol. NMR 2*, 661−665.
22. Marion, D. and Wuthrich, K. (1983) *Biochem. Biophys. Res. Commun. 113*, 967−974.
23. Ernst, R. R., Bodenhausen, G., and Wokaun, A. (1987) *Principles of Nuclear Magnetic Resonance in One and Two Dimensions*, pp 494−496, Clarendon Press, Oxford, England.
24. Bax, A., and Davis, D. G. (1985) *J. Magn. Reson. 65*, 355−360.
25. Ni, F. (1994) *Prog. NMR Spectrosc. 26*, 517−606.
26. Sklenar, V., Piotto, M., Leppik, R., and Saudek, V. (1993) *J. Magn. Reson. A 102*, 241−245.
27. Lippens, G., Dhalliun, C., and Wieruszeski, J.-M. (1995) *J. Biomol. NMR 5*, 327−331.
28. Baleja, J. D., Moult, J., and Sykes, B. D. (1990) *J. Magn. Reson. 87*, 375−384.
29. Moseley, H. N. B., Curto, E. V., and Krishna, N. R. (1995) *J. Magn. Reson., Ser. B 108*, 243−261.
30. Meyer, E. F., Clore, G. M., Gronenborn, A. M., and Hansen, H. A. S. (1988) *Biochemistry 27*, 725−730.
31. Polgar, L., Ed. *Mechanisms of Protease Action*, CRC Press, Roca Baton, FL.
32. Sardana, V. V., Wolfgang, J. A., Veloski, C. A., Long, W. J., Legrow, K., Wolanski, B., Emini, E. A., and LaFemina, R. L. (1994) *J. Biol. Chem. 269*, 14337−14340.
33. LaFemina, R. L., Bakshi, K., Long, W. J., Pramanik, B., Veloski, C. A., Wolanski, B. S., Marcy, A. I., and Hazuda, D. J. (1996) *J. Virol. 70*, 4819−4824.
34. Ogilvie, W., Bailey, M., Poupart, M.-A., Abraham, A., Bhavsar, A., Bonneau, P. R., Bordeleau, J., Bousquet, Y., Chabot, C., Duceppe, J.-S., Fazal, G., Goulet, S., Grand-Maître, C., Guse, I., Halmos, T., Lavallée, P., Leach, M., Malenfant, E., O'Meara, J. A., Plante, R., Plouffe, C., Poirier, M., Soucy, F., Yoakim, C., and Déziel, R. (1998) *J. Med. Chem. 40*, 4113−4135.
35. Stevens, J. T., Mapelli, C., Tsao, J., Hail, M., O'Boyle, D., II, Weinheimer, S. P., and Diianni, C. L. (1994) *Eur. J. Biochem. 226*, 361−367.
36. Wüthrich, K., Billeter, M., and Braun, W. (1984) *J. Mol. Biol. 180*, 715−740.
37. Nicotra, M., Paci, M., Sette, M., Oakley, A. J., Parker, M. W., Lo Bello, M., Caccuri, A. M., Federici, G., and Ricci, G. (1998) *Biochemistry 37*, 3020−3027.
38. Jones, T. R., Sun, L., Bebernitz, G. A., Muzithras, V. P., Kim, H.-J., Johnston, S. H., and Baum, E. Z. (1994) *J. Virol. 68*, 3742−3752.
39. Welch, A. R., McNally, L. M., Hall, M. R. T., and Gibson, W. (1993) *J. Virol. 67*, 7360−7372.
40. Burck, P. J., Berg, D. H., Luk, T. P., Sassmannshausen, L. M., Wakulchik, M., Smith, D. P., Hsiung, H. M., Becker, G. W., Gibson, W., and Villarreal, E. C. (1994) *J. Virol. 68*, 2937−2946.
41. Holwerda, B. C., Wittwer, A. J., Duffin, K. L., Smith, C., Toth, M. V., Carr, L. S., Wiegang, R. C., and Bryant, M. L. (1994) *J. Biol. Chem. 269*, 25911−25915.
42. McCann, P. J., III, O'Boyle, D. R., II, and Deckman, I. C. (1994) *J. Virol. 68*, 526−529.

BI980555V